

Inflammation as a Cancer Co-Initiator: New Mechanistic Model Predicts Low/Negligible Risk at Noninflammatory Carcinogen Doses

Dose-Response:
An International Journal
April-June 2019:1-12
© The Author(s) 2019
Article reuse guidelines:
sagepub.com/journals-permissions
DOI: 10.1177/1559325819847834
journals.sagepub.com/home/dos



Kenneth T. Bogen¹

Abstract

Linear-no-threshold (LNT) risk extrapolation has long been applied to estimate risks posed by low-level environmental carcinogen exposures, based on the 60-year-old multistage somatic mutation/clonal expansion (MSM) cancer theory. Recent evidence supports an alternative theory: Malignant tumors arise most efficiently from a stem cell that incurs requisite mutations and also is activated by inflammation to an epigenetically mediated and maintained state of adaptive hyperplasia (AH). This new inflammation-MSM (ISM) theory posits that inflammation-activated stem cells normally restricted to sites of injury-induced inflammation and tissue repair become uniquely susceptible to efficient carcinogenesis if normal post-inflammation AH termination is blocked by mutation. This theory posits that inflammation generally thus co-initiates cancer and transiently amplifies activated stem cells, implying that MSM theory (eg, the 2-stage stochastic “Moolgavkar, Venzon, Knudson [MVK]” model) is incomplete. Because inflammation dose–response typically is not LNT, the ISM theory predicts this is also true for most (perhaps all) carcinogens. The ISM (but not the MVK) model is shown to be consistent with recent data showing ~100% carcinoma incidence (but not DNA adducts) in livers of rats exposed to aflatoxin B₁ and was eliminated when that dose was co-administered with a highly potent anti-inflammatory agent. Experimental approaches to test ISM theory more robustly are discussed.

Keywords

biological mechanism, conditional multistage model, inflammation, low-dose nonlinearity, stem cells, cancer

Introduction

Linear-no-threshold (LNT) risk extrapolation has long been applied to estimate risks posed by low-level environmental (particularly by default for mutagenic) carcinogen exposures, based on the 60-year-old multistage somatic mutation/clonal expansion (MSM) theory of cancer.¹ First proposed and represented mathematically by Armitage and Doll in 1957,² the MSM theory overlaps most other current competing theories of cancer because the critical events it posits (namely, 2 or more critical oncogene mutations in a somatic stem cell, coupled if/as applicable with intrinsic and/or exposure-induced “promotion” by net proliferation of intermediate/premalignant cells) can also be induced or augmented by events posited as critical by those theories (eg, theories focusing on:³ oxidative stress, infection, an inflammatory microenvironment, defective wound healing, chromosome damage, genomic instability, and epigenetic dysregulation). Generalizing MSM theory and Knudsen’s related 2-mutation tumor suppressor inactivation model describing inherited susceptibility to

retinoblastoma,⁴⁻⁶ Moolgavkar, Venzon, Knudson (MVK) and colleagues represented the MSM model mathematically as a 2-stage doubly stochastic Poisson process (Figure 1, left) and fit this model well to many sets of experimental cancer bioassay and human cancer incidence data.⁷⁻¹⁷ Specifically, the MVK model assumes that a critical mutation can “initiate” any normal stem cell to yield a premalignant daughter cell, and an additional critical mutation in a premalignant cell can “complete” the process of neoplastic transformation to yield (possibly after some “lag” period) a malignant daughter cell. However, as previously discussed,^{3,18,19} experimental and

¹ 9832 Darcy Forest Drive, Silver Spring, MD, USA

Received 08 October 2018; received revised 07 April 2019; accepted 09 April 2019

Corresponding Author:

Kenneth T. Bogen, 9832 Darcy Forest Drive, Silver Spring, MD 20910, USA.
Email: ktbogen@icloud.com



Creative Commons Non Commercial CC BY-NC: This article is distributed under the terms of the Creative Commons Attribution-NonCommercial 4.0 License (<http://www.creativecommons.org/licenses/by-nc/4.0/>) which permits non-commercial use, reproduction and distribution of the work without further permission provided the original work is attributed as specified on the SAGE and Open Access pages (<https://us.sagepub.com/en-us/nam/open-access-at-sage>).

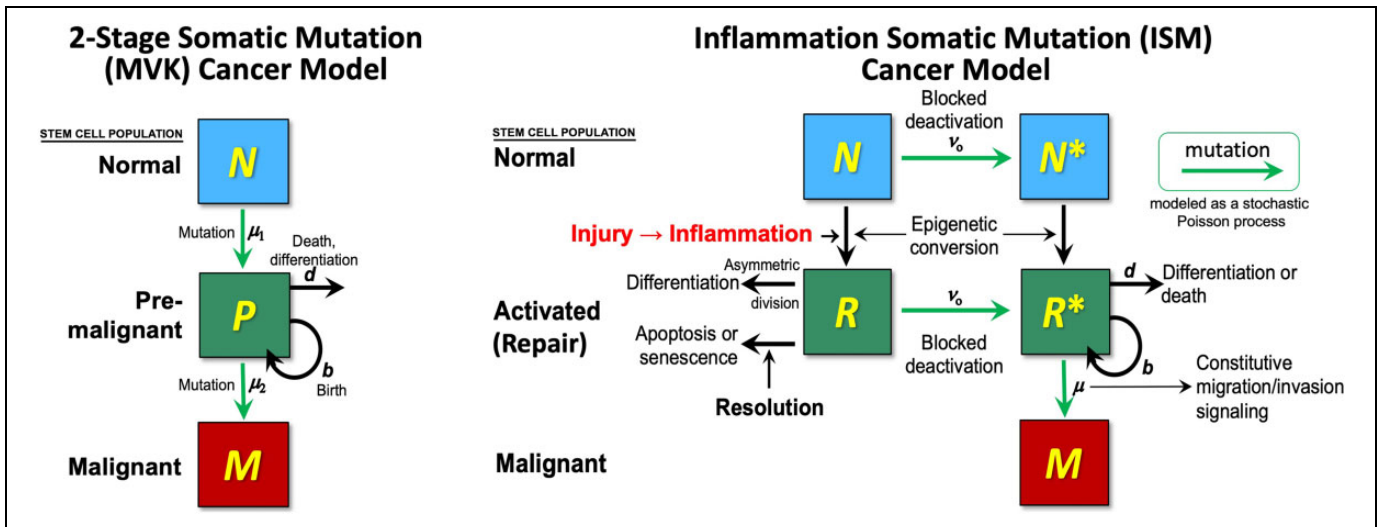


Figure 1. According to the 65-year-old 2-stage somatic mutation/clonal expansion theory of cancer and its more recent doubly stochastic Moolgavkar-Venzon-Knudsen (MVK) implementation (left), 2 critical mutations suffice to transform (at rate μ_1) any normal (N) stem cell into a premalignant stem cell (P), which may clonally proliferate, and (at rate μ_2) any P cell into an incipient malignant (M) cell. The ISM model (right) posits instead that cancer arises most efficiently only from a small subset of N -cells—those that have been recruited at a site of local tissue injury to undergo epigenetic reprogramming to become “repair-activated” stem (R) cells by inflammatory immune cells that normally and episodically accumulate at any such site to orchestrate the process of tissue repair. According to this model, a critical mutation incurred (at rate ν_c) by either an N or an R cell (transforming it into an N^* or R^* cell, respectively) that can block the pathway by which R cells in that specific tissue would otherwise normally deactivate (ie, revert into an N -cell, senesce, or die apoptotically, via signaling that normally accompanies tissue repair and resolution of inflammation at that site). The ISM model posits that a second critical mutation (incurred at rate μ) constitutively activates a migratory/invasive phenotype in R^* cells—a phenotype that otherwise normally requires continuous inflammation-related signals generated by immune cells while they detect unrepaired tissue damage.

clinical observations that appear to contradict MSM-based expectations have continued to generate interest in alternative ways to understand key events that typically cause cancer. Such observations include, for example,

- pronounced nonlinearity (rather than MVK-predicted linearity) of detailed low-dose dose-response relationships observed for tumors induced by the highly potent mutagen dibenzo[*a, l*]pyrene in the largest experimental cancer bioassay ever conducted (involving >40 000 animals)¹⁸ and
- reduction from nearly 100% (22/23) lifetime hepatocellular carcinoma (HCC) incidence observed by Johnson et al²⁰ in the first 2 groups of rats exposed during weeks 6 to 9 to a 200 $\mu\text{g}/\text{kg}/\text{d}$ gavage dose of the highly potent mutagen aflatoxin B₁ (AFB₁), to 0% (0/20) in a second group of AFB₁-treated rats that also were co-administered (and during week 5 preceded only by) 16.2-mg/kg/d of a highly potent anti-inflammatory, synthetic oleanane triterpenoid 1-[2-cyano-3-,12-dioxooleana-1,9(11)-dien-28-oyl]imidazole (CDDO-Im), which only partially reduced hepatocellular AFB₁-DNA adducts measured during and at the end of AFB₁ exposure.

An alternative to MSM theory is that dysregulated adaptive hyperplasia (DAH) is a general mechanism by which cancer typically arises in all tissues that contain or attract stem cells

involved in tissue repair-associated adaptive hyperplasia (RAH).^{3,19} According to that new theory, normal stem cells differ widely in the degree to which they are susceptible to critical mutation-induced generation of premalignant or malignant daughter cells, and more specifically that

1. only a stem cell specifically activated into an epigenetically mediated and maintained RAH state can generate a premalignant and subsequently a malignant daughter cell by accumulating (either prior or subsequent to RAH activation) as few as 2 respective critical mutations;
2. without such activation, any stem cell needs to accumulate at least 3 but more likely 4 or more mutations to generate a malignant neoplasm in vivo; and consequently
3. pathways involving RAH-activated stem cells are relatively efficient and prevalent pathways to cancer in all susceptible tissues of all higher animals.

The DAH theory implies that MSM theory is fundamentally incomplete by claiming that the most efficient pathway to a malignant phenotype in each tissue involves only its RAH-activated subpopulation of stem cells—that is, cells already epigenetically programmed to express a suite of capacities (eg, for invasive migration through tissue barriers, Warburg metabolic state conducive to cell proliferation, proliferation in a targeted niche, elicitation of vascularization, and so on) that normally contribute to tissue repair but which become

nonfunctional, uncontrolled, and persistent if normal RAH termination is blocked by a critical mutation that prevents terminal signal transduction.^{3,19} The DAH theory predicts that likelihood of cancer occurrence in each tissue by a given age is proportional to the time-weighted average (TWA) number of RAH-activated stem cells (rather than all stem cells) in that tissue by that age.³ Consistent with recent bioassay data mentioned earlier,²⁰ this theory also predicts that highly increased lifetime tumor incidence associated with short-term exposure to a sufficiently potent genotoxin can be prevented efficiently, or entirely, simply by blocking exposure-related inflammation and associated RAH activation, despite substantial, residual DNA damage.¹⁹

Here the DAH theory is first refined to specify that RAH activation of stem cells associated with tissue repair is triggered and later terminated specifically by cytokine signals released from local inflammation-associated immune cells that normally congregate at sites of tissue injury and mediate the process of tissue repair. This more refined interpretation, which shall be called the inflammation-MSM (ISM) theory of cancer, is next approximated mathematically, using an MVK-like model reinterpreted to involve ISM-specific model parameters and assumptions (Figure 1, right). The ISM model is then applied to show that, unlike the original MVK model representing the MSM theory, the ISM model readily explains very diverse, tissue-specific patterns of human cancer incidence and readily explains the bioassay data of Johnson et al.²⁰ The following 3 sections discuss: methods used for DAH-to-ISM theory refinement, mathematical ISM-model implementation, and ISM and MVK model fits to bioassay data; corresponding results obtained; and a discussion of dose–response and clinical implications as well as experimental approaches to test the ISM theory more rigorously.

Methods

Dysregulated Adaptive Hyperplasia-to-ISM Theory Refinement

Literature addressing interrelationships among the topics of inflammation, stem cell activation, tissue repair, and carcinogen/tumorigenesis was reviewed to identify a common mechanism by which stem cells typically are recruited to participate in tissue repair in ways that correlate with carcinogenesis and carcinogen exposure. This proposed mechanism was inferred from key conclusions of the review performed and then combined with the DAH theory to yield a more specific ISM theory positing how stem cells typically become activated into a normally transient RAH state that is (following the DAH theory^{3,19}) subject to mutation-associated dysregulation to yield a relatively efficient pathway to cancer (Figure 1, right). Plausibility of this mechanism was confirmed by identifying evidence that multiple carcinogens are well known to engage this same mechanism.

Representation of ISM Model and Fits to Cancer Incidence Data

To predict cancer risk in accordance with the ISM theory, the analytic solution to the MVK mathematical 2-stage (doubly stochastic Poisson-process) model of age-specific cancer incidence and cumulative cancer likelihood¹⁴ was adapted simply by applying a modified biological interpretation of MVK model parameters (see Results and Appendix A), recognizing that each MVK/ISM model fit obtained may be nonunique.¹⁵ Model plausibility was verified first by visual fits to diverse, tissue-, and sex-specific patterns of US Surveillance, Epidemiology, and End Results (SEER) program 2010 to 2014 cancer incidence data, for illustration focusing on the largest racial group (whites).²¹

The MVK and ISM model calculations and heuristic assessment of goodness-of-fit to Johnson et al.²⁰ study data on cumulative likelihood of HCC mortality in the 2 groups of male F344/NHsd rats (see Introduction) using P values (p_{KSI}) from Kolmogorov 1-sample tests,²² a 2-tailed upper 95% confidence bound on HCC incidence rate (0/20) observed in rats co-administered CDDO-Im in that study assuming Poisson-distributed sampling error,²³ and a 2-tailed Fisher exact test of homogeneity between historical HCC incidence rates in unexposed rats were performed using *Mathematica*[®] 11.3 software.²⁴ As summarized above (Introduction section), the Johnson et al.²⁰ rat study compared HCC mortality in 2 groups of AFB₁-exposed rats: those administered AFB₁ only (group 1) versus those co-administered the potent anti-inflammatory agent CDDO-Im (group 2). Thus, that study included no unexposed control group. The HCC mortality in unexposed male F344 rats was therefore estimated from National Toxicology Program (NTP) historical lifetime control data²⁵ and from similar historical age-specific control data summarized and modeled by Portier et al.²⁶ The MVK/ISM model fits to HCC mortality data assumed zero lag between incidence and fatality, in accordance with the observation that rat HCC tumors are generally fatal.²⁷

After in vitro cellular or in vivo exposure, 2 primary types of (after in vivo exposure, primarily but not exclusively hepatic) AFB₁-DNA adducts form, the most prevalent being relatively rapidly removed 8,9-dihydro-8-(*N*₇-guanyl)-9-hydroxyafatoxin (AFB₁-*N*₇-dG) DNA adducts, ~20% of which undergo imidazole ring opening that converts these to relatively stable and apparently irreparable AFB₁-formamidopyrimidine (AFB₁-FAPY) DNA adducts that are considered primarily responsible for AFB₁-associated (primarily GC→TA transversion) mutations.²⁷⁻⁴² After low-level exposure to AFB₁, the AFB₁-DNA adducts accumulate in approximately linear proportion to cumulative dose with AFB₁-FAPY adducts dominating ~72 hours after a single exposure and (presumptively or as measured) during intermittent, subchronic, or chronic exposure.^{33,40,43-45} The AFB₁-DNA adducts in turn induce mutations and (with possibly greater potency) mitotic recombination in roughly linear proportion to adduct load.⁴⁶⁻⁴⁹ The MVK model fit to male rat HCC data thus presumed that:

(1) AFB₁ acted to increase (for simplicity, equal) first and second mutation rates $\nu(t)$ and $\mu(t)$ (see Appendix A) over their background values in the absence of such exposure by an equal magnitude F proportional to dose both during and (because of AFB₁-FAPY adduct persistence) after AFB₁ exposure and (2) CDDO-Im acted to reduce F to values $f_2 F$ and $f_3 F$ during and after AFB₁ exposure, respectively, using corresponding fractions $f_2 = 0.31$ and $f_3 = 0.40$ measured by Johnson et al.²⁰ for liver AFB₁-FAPY adducts in rats co-administered CDDO-Im relative to adducts measured, respectively, during those 2 periods. Additionally, to minimize HCC incidence predicted under the AFB₁ + CDDO-Im protocol under assumptions plausibly consistent with MSM theory implemented by an MVK model, it was assumed that during AFB₁ exposure CDDO-Im acted on premalignant cells to reduce their birth rate $b(t)$ 1000-fold and increase their death rate $d(t)$ 10-fold relative to these rates without CDDO-Im co-exposure.

In contrast, the ISM model fit to data on HCC in male rats dosed only with AFB₁ presumed that: (1) during and after exposure AFB₁ acted to increase the effective rate of new premalignant-cell (R^* -cell) clone occurrence over its background rate $N(t)\nu(t)$ without AFB₁ exposure (see Appendix A) and (2) before and during AFB₁ exposure CDDO-Im acted to reduce or prevent any AFB₁-related increase in the rate of new R^* -cell clone occurrence above $N(t)\nu(t)$ absent AFB₁-exposure via its ability to reduce or block inflammation and (posited) associated R -cell activation that (absent such suppression) is triggered by AFB₁-induced liver injury. Thus, that fit assumed CDDO-Im exposure acted to reduce the increased rate $r = (1+s)r_0$ of HCC incidence and, as noted above, HCC mortality observed only after exposure to AFB₁ (eg, with $s \gg 0$), relative to the corresponding background rate r_0 , by reducing s to a value (as low as zero) determined by the relative potency at which AFB₁ exposure can augment baseline rates of $N(t)\nu(t)$ and $\mu(t)$ absent AFB₁ exposure.

Results

The ISM Theory of Cancer

The DAH theory of tumorigenesis did not specify a common mechanism by which stem cells in different tissues are recruited into and subsequently terminated from an activated state of RAH. Concerning such a mechanism, literature reviewed in Supplementary Materials Appendix S1 supports the following conclusions

- *Two oncogene/tumor-suppressor mutations may not typically suffice to cause cancer.* Although complete deactivation of an oncogene, such as the retinoblastoma gene (*RBI*), may suffice or tend to generate relatively rare hereditary tumors in accordance with Knudsen's 2-mutation model and the related MVK model, complete mutational and/or epigenetic deactivation of 3 or more oncogenes appears to be required to generate

malignant tumors—even those associated with *RBI* deactivation, which (in common with deactivation of certain other oncogenes) now is known to trigger chronic inflammation via inducing aberrant inflammatory cytokine release (see Appendix S1.A).

- *Inflammation activates stem cells to participate in tissue repair.* The inflammatory response to tissue injury involving locally recruited immune cells (eg, macrophages and neutrophils) as well as local and (after more severe trauma) other neuroendocrine cells that jointly and actively coordinate highly orchestrated, cytokine-mediated processes of tissue repair. In tissue repair, local stem cells are activated epigenetically to dedifferentiate, initiate Warburg metabolism (characterized by lactate-generating aerobic glycolysis that facilitates nucleotide, amino acid, and lipid biosynthesis required for proliferating cells of any type, whether engaged in development, tissue renewal, tissue repair, immune response, or neoplastic growth), migrate to and within sites of damaged tissue, proliferate, and help trigger vascularization that supplies required oxygen and nutrients. Normally, the repair process terminates with a coordinated resolution of inflammation in which activated stem cells are prompted to undergo either epigenetic deactivation and redifferentiation, senescence, or apoptosis within repaired tissue (see Appendix S1.B).
- *Aging-associated senescence reduces stem-cell activation capacity.* During adult aging over time, the prevalence of stem cells capable of participating in tissue repair declines and the prevalence of senescent cells incapable of participating in tissue repair increases (see Appendix S1.C).
- *Cytotoxicity-induced inflammatory effects of carcinogens are consistent with a co-initiating role of inflammation.* A co-initiating role of localized injury-related inflammation in carcinogenesis is supported by observations that inflammation is not simply a tumor-promoting hallmark of the tumor microenvironment with recurrent epidemiological links to elevated cancer risk. Inflammation is also an end point consistently observed to be induced by carcinogenic exposures to nongenotoxic cancer promoters (such as phorbol esters, implanted “solid state” foreign bodies, and certain nongenotoxic fibers and particles) as well as genotoxic carcinogens (such as cigarette smoke, ozone, arsenic, nickel, hexavalent chromium, organic alkylating chemicals, mutagenic polycyclic aromatic hydrocarbons, and ionizing radiation; see Appendix S1.D).

These conclusions are consistent with a modified version of the DAH theory specifying that stem cell activation to participate in RAH is triggered specifically by cytokine and/or cell contact signals from immune cells (possibly in coordination with local neuroendocrine cells). These immune cells are characteristically involved in the normally transient process of local inflammation that actively mediates tissue repair following

local tissue injury. This more specific ISM theory of cancer (Figure 1, right) implies that such inflammation is not merely a cancer promoter (by acting, as long recognized, via various mechanisms to increase the net proliferation of premalignant and incipient malignant cells). The ISM theory of cancer also implies that inflammation also is a cancer co-initiator by acting to increase the time-integrated population of repair-activated stem cells, which according to ISM theory generates cancer most efficiently in each affected tissue and so primarily determine average tissue-specific rates of cancer incidence.

The ISM Model Representation and Fits to Cancer Incidence Data

The MVK and ISM models are structurally (ie, mathematically) identical, but their parameters represent fundamentally different biological interpretations of critical events posited to be required for efficient carcinogenesis (see Appendix A). Both models assume that tumor likelihood is driven by an accumulation of critical mutations in a total of $N(t)$ stem cells at time t and amplified by premalignant cell clonal expansion. However, as explained in the Appendix A, the ISM model effectively conditions $N(t)$ to represent not all stem cells but only those that are RAH-activated by inflammation-associated immune cells in response to local tissue damage. The tissue-specific integrated rate $N(t)\nu(t)$ over time t is assumed to represent an accumulation of critical mutations at rate $\nu(t)$ in all stem cells. However, this integrated rate represents accumulation of a critical mutation that occurs only in an inflammation-activated subset of all stem cells and that acts in those cells to block normal post-repair termination of their activated state. In this way, the ISM model interprets tissue injury-associated inflammation to (1) be a requisite step in a relatively efficient (and thus likely dominant) pathway to cancer; (2) increase cancer likelihood in proportion to the TWA number of inflammation-activated stem cells; and consequently (3) act together with critical mutations as a co-initiator of cancer.

Model Fits to Cancer Data

The NCI SEER data on US white male and female age-specific background incidence of 4 types of cancer (urinary bladder, lung and bronchus, thyroid, and leukemia), which illustrate different corresponding patterns of age-specific incidence exhibited by different types of cancer in the United States, are plausibly consistent with corresponding MVK/ISM model fits to those data sets (Supplementary Material, Table S1 and Figures S1–S4). Both the MVK and the ISM models are expected to reflect gradual or abrupt changes in average stem cell population size over different age ranges, which may explain the patterns observed for male and female bladder, lung, and thyroid cancer incidence. However, the clearly bimodal nonmonotonic pattern observed for male and female leukemia incidence appears more difficult to reconcile with an MVK model parameter interpretation. The spike in US male and female childhood (primarily acute myeloid or lymphocytic)

leukemia incidence observed to peak at about 2.5 years of age (Figure S4, Supplementary Materials) has been considered primarily due to unidentified causes.⁵⁰ However, the recently proposed “delayed-infection” explanation of this childhood spike in leukemia and of its increasing incidence in more developed countries⁵¹ appears more consistent with an ISM-model parameter interpretation.

Both MVK and ISM models fit to data on HCC incidence in AFB₁-exposed rats studied by Johnson et al²⁰ alone (in Group 1) or coadministered together with the potentially anti-inflammatory (ai) triterpene CDDO-Im (in Group 2) are summarized in Table 1 and compared in Figure 2. As expected, although the MVK and ISM model fits to data (ie, to the plotted step function) on HCC mortality in group 1 rats implemented the different, model-specific sets of parameters listed in Table 1, the 2 fits virtually overlie one another and provide equally good fits to those data ($P_{KSI} > .999$). A baseline MVK model (solid blue curve labeled MVK₀ in Figure 2) appears reasonably consistent with an age-specific model of HCC in historical control male F344 rats fit by Portier et al²⁶ (blue dashed curve in Figure 2), which in turn exhibited a lifetime HCC incidence at week 104 approximately equal to that exhibited in more recent NTP historical control male F344/NHsd rats ($P = .51$ by 2-tailed Fisher exact test).²⁵

The MVK model was also applied as described in Methods and Table 1 to predict the maximum reduction in HCC mortality in group 2 rats exposed to both AFB₁ and CDDO-Im. This application was consistent with MVK modeling assumptions that (as described in Methods section) CDDO-Im acted to reduce both AFB₁-induced mutations proportional to AFB₁-adduct loads measured during and at the end of joint exposure and premalignant cell net proliferation during that exposure. The resulting prediction (red dashed curve labeled MVK_{ai} in Figure 2) shows that the MVK approach to modeling this scenario reduced predicted HCC mortality to 45.8% at week 104, and thus clearly failed to reduce mortality below the (16.8%) upper 95% confidence bound (horizontal black dashed line in Figure 2) on the (0/20) fraction of rats observed with HCC at week 104 in this experimental group. That is, the MVK_{ai} model fit (representing the greatest reduction in HCC incidence consistent with MVK-model assumptions applied to group 2 rats) is significantly inconsistent with the observed data on HCC mortality in group 2 rats.

In contrast, an ISM model fit consistent with modeling assumptions for group 2 rats assumes that CDDO-Im exposure reduces or perhaps even totally blocks epigenetic conversion of both normal and any critically mutated stem cells to an RAH-activated state. According to the ISM model, this state must be engaged for a critically mutated stem cell to contribute efficiently to increased cancer risk. The ISM model (black dashed curve labeled ISM_{ai} in Figure 2) thus explains the observed HCC rate of 0/20 in this experimental group by assuming that coexposure to CDDO-Im in group 2 rats reduced HCC mortality at week 104 substantially below that observed in group 1 rats exposed only to AFB₁—that is, to below the upper 95%

Table 1. MVK/ISM Model Fits to Johnson et al data.^{20,a}

Data Set	Model ^b	Parameter ^b	Time interval (i)	Interval end ^b (t_i), Weeks	Scaled factor ^c = SF	Scale, ^c = S_i	
AFB ₁ only (Group 1)	MVK	$N(t)$	$\nu(t)$	1, 2, 3	6, 10, 104	10/52	1, 42.19, 42.19
		$b(t)$		1, 2, 3	6, 10, 104	1/52	6, 5.66436, 3.7895
		$d(t)$		1, 2, 3	6, 10, 104	1/52	1, 1, 1
		$\mu(t)$		1, 2, 3	6, 10, 104	$10^{-5}/52$	1, 42.19, 42.19
AFB ₁ only (Group 1)	MVK _{pp}	$N(t)$	$\nu(t)$	1, 2, 3	6, 10, 104	10/52	1, 1, 1
		$b(t)$		1, 2, 3	6, 10, 104	1/52	6, 66.4, 8.41
		$d(t)$		1, 2, 3	6, 10, 104	1/52	1, 1, 1
		$\mu(t)$		1, 2, 3	6, 10, 104	$10^{-5}/52$	1, 1, 1
AFB ₁ only (Group 1)	ISM	$N(t)$	$\nu(t)$	1, 2, 3	6, 10, 104	10/52	1, 1812.1, 1812.1
		$b(t)$		1, 2, 3	6, 10, 104	1/52	6, 6, 4.122
		$d(t)$		1, 2, 3	6, 10, 104	1/52	1, 1, 1
		$\mu(t)$		1, 2, 3	6, 10, 104	$10^{-5}/52$	1, 1, 1
AFB ₁ + CDDO-Im (Group 2)	MVK _{ai}	$N(t)$	$\nu(t)$	1, 2, 3	6, 10, 104	10/52	1, f_2 42.19, f_3 42.19
		$b(t)$		1, 2, 3	6, 10, 104	1/52	6, 10^{-3} , 3.7895
		$d(t)$		1, 2, 3	6, 10, 104	1/52	1, 10, 1
		$\mu(t)$		1, 2, 3	6, 10, 104	$10^{-5}/52$	1, f_2 42.19, f_3 42.19
AFB ₁ + CDDO-Im (Group 2)	MVK _{ppai}	$N(t)$	$\nu(t)$	1, 2, 3	6, 10, 104	10/52	1, 1, 1
		$b(t)$		1, 2, 3	6, 10, 104	1/52	6, 1 to 30^d , 4.122
		$d(t)$		1, 2, 3	6, 10, 104	1/52	1, 1, 1
		$\mu(t)$		1, 2, 3	6, 10, 104	$10^{-5}/52$	1, 1, 1
Historical control rats	MVK & ISM	$N(t)$	$\nu(t)$	1	104	10/52	1, 1, 1
		$b(t)$		1	104	1/52	6, 6, 4.122
		$d(t)$		1	104	1/52	1, 1, 1
		$\mu(t)$		1	104	$10^{-5}/52$	1, 1, 1

Abbreviations: AFB₁, aflatoxin B₁; CDDO-Im, 1-[2-cyano-3,12-dioxooleana-1,9(11)-dien-28-oyl]imidazole; HCC, hepatocellular carcinoma; ISM, Inflammation-MSM; MSM, multistage somatic mutation/clonal expansion (MSM); MVK, Moolgavkar-Venzon-Knudsen.

^aThe Johnson et al²⁰ data pertain to HCC mortality in male F344/NHsd rats administered 200 $\mu\text{g}/\text{kg}/\text{d}$ AFB₁ by gavage (without vs. with CDDO-Im) during weeks 6–9 vs. in historical control male F344 rats.

^bMVK and ISM models and parameters defined in the Appendix; ai subscript on MVK model denotes model fit to data on group 2 rats co-exposed to anti-inflammatory agent CDDO-Im. In your $b_2(t)$ during MVK_{pp} and MVK_{ppai} denote MVK models fit under the (biologically implausible) assumption that AFB₁ acts to increase HCC risk as a pure promoter, that is, by increasing the P-cell birth rates $b(t)$ during and after AFB₁ exposure without affecting rates at which critical mutations accumulate; the MVK_{ppai} fit assumes that AFB₁-induced elevations in $b(t)$ are reduced during and after CDDO-Im co-exposure. Age interval i extends from t_{i-1} to t_i , where $t_0 = 0$.

^cParameter value during age interval i is equal to the product $\text{SF} \times S_i$. The MVK model was applied assuming that co-administration of CDDO-Im during time interval $i = 2$ acts to reduce birth rate $b_2(t)$ 1000-fold, to increase death rate $d_2(t)$ 10-fold, and during intervals $i = 2$ and $i = 3$ to reduce both mutation rates $\nu_i(t)$ and $\mu_i(t)$ to fractions $f_2 = 0.31$ and $f_3 = 0.40$ of those rates, respectively, compared to corresponding rates in rats exposed to only to AFB₁ (see Methods section).

^dSee Figure 3.

confidence bound on the true but unknown fraction consistent with the observed response rate of 0/20 and possibly as low as the historical control rate of 4/699 = 0.57% at week 104 (black solid point in Figure 2).

An MVK model was found to provide a good fit to all of the Jones et al²⁰ bioassay data only under the assumption that AFB₁ acts as a “pure promoter,” that is, acts to increase HCC in group 1 rats only by increasing P-cell birth rates b_2 and b_3 during and after AFB₁ exposure, respectively, without affecting rates of critical mutation (Table 1; Figure 3). Under this assumption, a good ($P_{KS1} = .939$) MVK fit to group-1 rat data is also consistent with the observed lack of any HCC in group 2 rats if CDDO-Im acted to reduce the birth-rate elevation caused by AFB₁ (Table 1; Figure 3). However, because AFB₁ is one of the most potently mutagenic liver carcinogens, the assumption that AFB₁ increases HCC risk only by acting as a cancer promoter without any contribution from AFB₁-induced mutations is not a biologically plausible application of the MVK model.

Discussion

Both MVK and ISM models provided virtually identical good fits to HCC time-to-tumor data for 23 rats from group 1 of the Johnson et al²⁰ study (Figure 2), which were administered AFB₁ for 4 weeks during weeks 6 to 9, followed for up to 2 years, and observed to have a 22 of 23 (ie, nearly 100%) incidence of HCC. However, it was found that no MVK model plausibly predicts the observation that HCC was not detected in any of the rats from group 2 of that study, which were exposed to AFB₁ for 4 weeks as in group 1 but also were co-administered CDDO-Im (including for one week just prior to AFB₁ exposure). Although Johnson et al²⁰ concluded that absence of any observed cancer in their group 2 rats “requires a concept of a threshold for DNA damage for cancer development,” they proposed no specific plausible mechanism by which such a genotoxicity threshold might operate. In contrast, the proposed ISM model requires no such threshold, is consistent with all the data obtained from that study and is supported

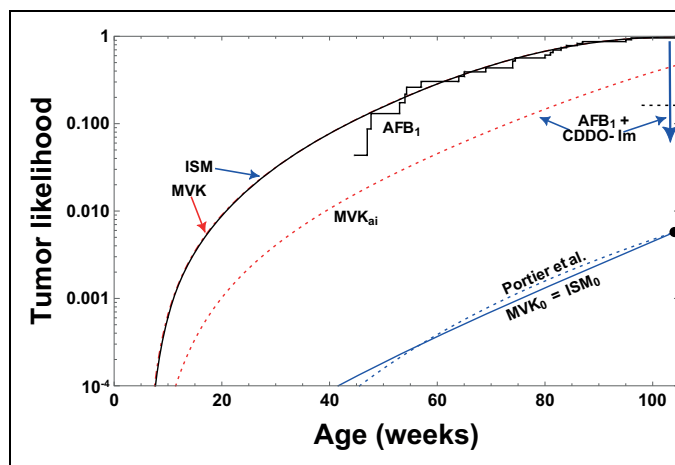


Figure 2. Moolgavkar-Venzon-Knudsen (MVK) and inflammation-multistage somatic mutation/clonal expansion (ISM) model predictions (red dot-dashed and solid black curves, respectively) are summarized in Table 1 compared to 2-year bioassay data reported by Johnson et al.²⁰ On cumulative hepatocellular carcinomas (HCC) incidence (step function) in 23 male F344 rats exposed for 4 weeks starting in week 6 (at ~ 85 g body weight) to 200 $\mu\text{g/day}$ (~ 2.35 mg/kg/day) of aflatoxin B₁ (AFB₁) by gavage ($n = 23$) and in 20 male F344 rats similarly AFB₁ exposed together with 30 μmol (16.2 mg/kg) of the potentially anti-inflammatory (ai) triterpene 1-[2-cyano-3-,12-dioxooleana-1,9(11)-dien-28-oyl]imidazole (CDDO-Im) 3 times/week for 5 weeks starting at week 5. Also shown is historical control background lifetime HCC incidence rate in male F344/NHsd rats ($r_0 = 4/669$, solid point) reported by the National Toxicology Program (NTP),²⁵ an MVK model (denoted MVK₀) fit conditioned on r_0 at week 104 (blue curve), the age-specific model (blue dotted curve) fit by Portier et al.²⁶ to historical control HCC incidence data for male F344 rats ($18/2670 = \sim r_0$ [$P = .51$ by Fisher exact test], here scaled exactly to r_0 at 104 weeks), and the upper 2-tail 95% confidence bound (equal to 16.8%) on observed HCC mortality risk (0/20) in rats exposed to AFB₁ + CDDO-Im.

by mechanistic and biologically pertinent data from studies reviewed in Appendix S1 of Supplementary Materials that accompany this article. A good MVK-model fit to HCC data from both groups of rats studied by Johnson et al.²⁰ could be obtained when AFB₁ was assumed to increase HCC risk by a purely promotional (ie, nongenotoxic) mode of action (Table 1; Figure 3). A previous study¹⁸ similarly reported that good MVK model fits to cancer bioassay data obtained after juvenile exposure to a potentially mutagenic carcinogen could be obtained only if a purely promotional (nongenotoxic) mode of action was assumed. That study compared good MVK and ISM-like model fits to highly detailed dose–response data on incidence of liver and stomach tumors from the ED₀₀₁ study involving >40 000 trout exposed as juveniles to dibenzo[*a,h*]pyrene (DBP), the most potentially mutagenic carcinogen.¹⁸ Good MVK-model fits to cancer bioassay data obtained using parameter values that assume a purely nongenotoxic mode of action clearly are not biologically plausible for data involving exposure to highly potentially mutagenic carcinogens such as AFB₁ and DPB.

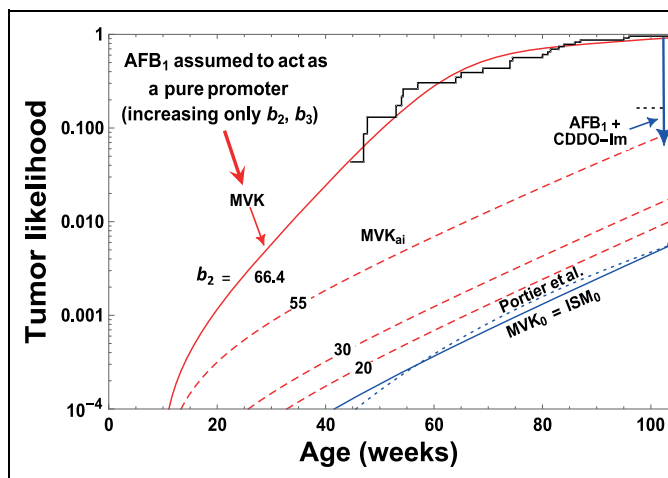


Figure 3. A good fit by the Moolgavkar-Venzon-Knudsen (MVK_{pp}) model shown by Johnson et al.²⁰ Data on hepatocellular carcinoma (HCC) in rats exposed only to aflatoxin B₁ (AFB₁; red curve) represent an MVK model in which AFB₁ acts to increase hepatocellular carcinoma (HCC) risk only as a “pure promoter” (ie, by increasing only P -cell birth rates b_2 and b_3 during and following, respectively, the period of AFB₁ exposure, without any effect on mutation rates μ_{11} and/or μ_{12}). Under this biologically implausible assumption, absence of observed HCC among 1-[2-cyano-3-,12-dioxooleana-1,9(11)-dien-28-oyl]imidazole (CDDO-Im) co-exposed rats is explained by corresponding MVK_{ppai} model fits shown which assumes CDDO-Im acts to reduce the amount of AFB₁ which is assumed to increase P cell birth rates. Specifically, the red-dashed curves show MVK_{ppai} fits using b_2 values less than that used to generate the red curve fit to the data on increased HCC incidence among AFB₁-exposed rats.

The proposed ISM model adapts the MSM/MVK model simply by conditioning it on an additional assumption that cancer in any specific tissue typically arises not from just any stem cell in that tissue but rather only from those that (triggered by signals from inflammatory immune cells responding to local tissue injury) are activated into an epigenetically mediated and maintained state of adaptive, tissue repair–directed hyperplasia. According to this theory, if such activation is blocked (eg, by suppressing inflammation that otherwise normally follows tissue damage), cancer formation will be suppressed greatly or blocked there, even after exposure to a potentially genotoxic carcinogen such as AFB₁ as was observed in the study by Johnson et al.²⁰ Efficient suppression of injury-related inflammation, however, would also be expected to hinder or block efficient injury repair.

Exposure to a genotoxic carcinogen at levels associated with observed significant elevations in cancer risk in a given tissue may, perhaps typically, also be accompanied by associated cytotoxic tissue damage sufficient to generate some (even low) level of inflammation in that tissue (see Appendix S1, Supplementary Materials). To this extent, in contrast to MSM/MVK theory, the ISM theory implies that increased cancer risks associated with exposures even to genotoxic carcinogens are expected to exhibit the same sorts and magnitudes of low-dose dose-response nonlinearity as those associated with the

induction of inflammation in response to local tissue injury. The ISM theory also predicts that such increased risks can in general be mitigated and perhaps blocked by suppressing or blocking corresponding local injury-associated inflammation, albeit at a likely cost of hindering or preventing efficient tissue repair. Moreover, inflammation per se tends to generate characteristic mutation spectra in affected tissues.⁵²⁻⁵⁵ To the extent that inflammatory mutation spectra differ from those characteristics of spontaneous tumors, the ISM theory would thus also predict a characteristic difference in mutation spectra in spontaneous tumors versus those associated with genotoxic chemical exposure. A recent analysis of published studies involving 45 genotoxic carcinogens studied, 13 mammalian models, and a broad range of tumor types has shown that there is just such a characteristic difference in mutagenic spectra for spontaneous versus chemically induced tumors.⁵⁶

Consequently, the ISM theory fundamentally challenges not only current default LNT dose–response assumptions for genotoxic carcinogens but also currently proposed mode-of-action frameworks and related toxicogenomics strategies to facilitate environmental carcinogen risk assessment.⁵⁷ As such, the ISM theory merits future rigorous experimental tests of the magnitude of low-dose dose–response nonlinearity it may imply for increased cancer risks posed by exposures to AFB₁ and for the extent to which this theory may apply to a broad range of genotoxic environmental carcinogens besides AFB₁, different tissues in addition to liver, and of different sex/strain/species combinations besides male F344 rats. For example, to determine more powerfully whether HCC mortality in group 2 rats of a Johnson et al²⁰-type study design is actually reduced to the historical control rate in male F344 rats, no rats with HCC at week 104 would need to be observed out of a total of ~250 (not just 20) group 2 rats, since rates of 4 of 699 and 0 of 250 have very similar upper 2-tail 95% confidence bounds (~1.5%). Likewise, a similar study design could be used to investigate whether CDDO-Im co-exposure effects a similar substantial reduction in or ablation of increased cancer incidence induced by other genotoxic carcinogens at other tissue sites and in other sex/strain/species combinations.

More generally, the ISM theory predicts that increased cancer risk above the baseline rate in any tissue at age t will always be proportional to the TWA number of repair-activated stem cells in that tissue by time t . Although relatively labor-intensive, methods for tissue-specific *in situ* localization of small subsets of quiescent stem cells⁵⁸ could be adapted to test this prediction. Specifically, such methods could be used to identify and measure tissue-specific densities of activated quiescent stem cell progeny or other activated forms of stem cells known to be recruited to participate in injury repair (eg, endothelial progenitor cells, mesenchymal stem cells, very small embryonic-like stem cells).⁵⁹ These methods could be compared after experimental tissue injury versus during/after genotoxic carcinogen exposure. Ultimately, however, new developments in real-time bioimaging^{60,61} could be adapted to allow more efficient estimation of the number of inflammation-

activated, repair-directed stem cells in each tissue of interest during the entire course of experimental carcinogenesis both with and without suppressed inflammation. Such adaptation could enable direct, rigorous tests of the ISM theory.

Finally, if true, the ISM theory will have important applications to the design of efficient cancer risk mitigation strategies in contexts concerning environmental health, occupational health, and clinical treatment. Specifically, the ISM theory predicts that increased risk of cancer is imposed most efficiently (ie, potently) by genotoxic agents at dose levels that both injure a tissue and mutate stem cells in that tissue that are also (or are likely to become) activated to help repair that tissue. This theory predicts that when acute- or short-term exposure to potentially cytotoxic levels of an environmental- or treatment-related genotoxic carcinogen (or any other source of tissue injury associated with elevated cancer risk) is known or predicted to occur, prophylactic (ideally approximately concurrent) administration of a potent anti-inflammatory agent such as CDDO-Im to the affected tissue will most efficiently reduce (perhaps even ablate) any increased associated cancer risk that otherwise might be expected to arise from such an exposure. Such applications might be particularly effective at mitigating increased cancer risk after chemotherapy-related, accidental, or unavoidable exposure to any cytotoxic dose of a genotoxic carcinogen. For example, such an approach might reduce treatment-related risks of subsequent secondary tumor formation or radiogenic cancer risks to astronauts outside low-earth orbit who encounter cytotoxic galactic-cosmic-ray or solar-particle events.

Appendix A

Mathematical Representation of ISM Model

The inflammation-multistage somatic mutation/clonal expansion (ISM) model adapts the Moolgavkar, Venzon, Knudson (MVK) model¹⁴ (Figure 1, left) that involves 5 parameters—here denoted: $N(t)$ (the number of normal stem cells at risk in a tissue at time t), $\nu(t)$ (the rate at time t at which any N cell incurs a somatic mutation that increments the population of pre-malignant cells $P(t)$ by one), $\mu(t)$ (the rate at time t at which any P cell incurs a somatic mutation that yields a new malignant or M cell), and $b(t)$ and $d(t)$ (the rates at which P cells proliferate, and die or differentiate, respectively, at time t)—as follows. The MVK model thus represents the occurrence of new P -cell clones as a Poisson process driven by rate $N(t)\nu(t)$, and the occurrence of new M cells as a doubly stochastic nonhomogeneous Poisson process driven by rate $P(t)\mu(t)$. In contrast, the ISM model (Figure 1, right) assumes the role played by $P(t)$ in the MVK model in each tissue is instead played only by a critically mutated subset $R^*(t)$ of all (ie, $R(t) + R^*(t)$) “repair-activated” stem cells, that is, stem cells engaged an epigenetically mediated and maintained activated state of tissue repair-associated adaptive hyperplasia (RAH) triggered by injury-associated inflammation. (The effect of this critical mutation, here and on the right side of Figure 1 denoted by

an asterisk, is defined below.) R cells are assumed to divide asymmetrically to yield either partially or terminally differentiated cells as long as local immune cells continue to signal (through direct contact or via one or more locally released cytokines) that additional R -cell progeny are required for tissue repair. Completion of tissue repair triggers resolution of local inflammation, which is mediated by a corresponding termination (ie, deactivation) signal (and/or cessation of “continued-repair” signaling) that normally is transduced highly efficiently by R cells resulting in apoptosis or senescence. However, a critical somatic mutation, incurred at rate $\nu_o(t)$, is assumed to block the ability of any R (or N) cell in a tissue to transduce this termination signal (eg, by inducing sustained autonomous “continued-repair” signal transduction), thereby converting that R cell into an R^* cell (or likewise converting that N cell into an N^* cell, which if RAH-activated becomes an R^* cell).

The ISM model presumes that $R(t) = f(t) N(t)$ and $R^*(t) = f(t) N^*(t)$, where $f(t)$ denotes the fraction of all normal stem (ie, $N + N^*$) cells that at time t are activated to a state of RAH, which in each tissue $f(t)$ typically has a relatively small (eg, $\leq 0.1\%$) characteristic background TWA value that occasionally increases transiently but perhaps substantially by inflammatory immune cells responding to tissue damage. This model also posits that if tissue injury is sufficiently extensive and/or local R -cell density is inadequate to effect repair, immune cells associated with local inflammation release 1 or more specific cytokine signals that induce and guide R cells to migrate (if necessary, invasively) to sites of damaged tissue of types specifically recognized by those R cells. It is further assumed that any R^* cell can acquire, at rate $\mu(t)$, an additional critical mutation that constitutively activates migration-inducing signal transduction in that R^* cell (and thereby transforms that R^* cell into an M cell, ie, into an incipient cancer stem cell), resulting in invasive/metastatic behavior and subsequent colonization of distant tissues with surface characteristics sufficiently similar to those normally recognized by the parent R cell in response to migration-eliciting cytokine signaling. The stochastic rate at which $R^*(t)$ increases over time is approximated as $\nu_o(t) R(t) + f(t) N^*(t) = 2\nu_o(t) f(t) N(t) = \nu(t) N(t)$, where $\nu(t) = 2\nu_o(t) f(t)$ and $N(t)$ is assumed to decrease over time t due to stem cell senescence during adulthood. Consequently, although the ISM and MVK model structures are mathematically identical, they reflect profoundly different biological interpretations of the driving rate $N(t)\nu(t)$ of the doubly stochastic Poisson process that both models use to represent the generation of new M cells. The MVK model presumes this rate in each tissue is proportional to the TWA number of all stem cells in that tissue, whereas the ISM model presumes rate is proportional to the TWA number of only those stem cells that are induced to undergo epigenetic conversion into an RAH-activated state by immune cells participating in tissue injury-associated inflammation.

Although not otherwise addressed in the present study, the ISM model also posits that new characteristically benign tumor (B) cells arise from a process parallel to that summarized in Figure 1, except that benign tumorigenesis is assumed to be

initiated not by tissue injury-associated inflammation but instead when a normal stem cell (N) is triggered by local noninjury-related (eg, mechanical irritation, sublethal cytotoxic, or metabolic-demand-associated) stress signals to undergo an epigenetic transformation into a cell engaged in state of relatively slow, tissue-enlarging protective adaptive hyperplasia (PAH), denoted as a P cell. As previously proposed,^{3,19} it is assumed that any such P cell may acquire a critical somatic mutation that blocks its normal ability to transduce a PAH-deactivation signal (ie, a signal that normally detects cessation of PAH-inducing stress) and so transforms that cell into a P^* cell that slowly generates new P^* cells only adjacent to itself or to its daughter P^* cells. A second critical mutation is assumed to confer on any P^* cell the ability to proliferate beyond its local tissue matrix, transforming that cell into a B cell, which likewise is assumed to generate new B cells only adjacent to itself or to its daughter B cells.

The MSM/MVK and ISM models thus each describe 2-stage (2-mutation) pathways posited to explain tumor occurrence. The MSM/MVK theory posits that 2 critical mutations typically are sufficient to generate all types of tumors other than those associated with relatively rare hereditary defects that greatly increase tumor risk and that stochastic net proliferation of premalignant stem cell clones amplifies the risk of tumor occurrence. Although the ISM theory also posits that 2 critical mutations typically are sufficient to generate all nonhereditary tumors, it additionally imposes a condition that each critical mutation must occur in a stem cell that has undergone (or will later undergo) epigenetically mediated RAH activation by immune cells associated with local inflammation due to tissue injury, unless that condition is satisfied via accumulation of one or more additional critical mutations that confer an epigenetic profile associated with an RAH-like phenotype (ie, via a k -stage MSM/MVK-like process with $k \geq 3$). According to the ISM theory, the most efficient pathway to cancer is thus one in which $k = 2$ and 1 of the 2 posited sufficient/critical mutations acts to prevent stem cell RAH-state termination that normally accompanies resolution of local injury-associated inflammation and tissue repair.

A recent alternative to MSM theory posits that the likelihood of cancer occurrence is determined not only by accumulation of critical mutations in stem cells but also by accumulation of stem cell divisions per se.⁶² The ISM model summarized above is far more specific than such a theory and offers a more efficient explanation of the striking cancer bioassay data reported by Johnson et al²⁰ to which MVK- and ISM-model fits are compared herein.

Acknowledgments

Comments and suggestions that anonymous reviewers provided are gratefully acknowledged.


Declaration of Conflicting Interests

The author(s) declared no potential conflicts of interest with respect to the research, authorship, and/or publication of this article.

Funding

The author(s) received no financial support for the research, authorship, and/or publication of this article.

ORCID iD

Kenneth T. Bogen  <https://orcid.org/0000-0001-5795-4612>

Supplemental Material

Supplemental material for this article is available online.

References

- Bogen KT. Unveiling variability and uncertainty for better science and decisions on cancer risks from environmental chemicals. *Risk Anal.* 2014;34(10):1795-1806. doi:10.1111/risa.12290.
- Armitage P, Doll R. A two-stage theory of carcinogenesis in relation to the age distribution of human cancer. *Br J Cancer.* 1957;11(2):161-169.
- Bogen KT. Efficient tumorigenesis by mutation-induced failure to terminate microRNA-mediated adaptive hyperplasia. *Medical Hypoth.* 2013;80(1):83-93. doi:10.1016/j.mehy.2012.10.017.
- Knudson AG Jr. Mutation and cancer: statistical study of retinoblastoma. *Proc Natl Acad Sci USA.* 1971;68(4):820-823.
- Knudson AG. Two genetic hits (more or less) to cancer. *Nature Rev Cancer.* 2001;1(2):157-62. doi:10.1038/35101031.
- Chial H. Tumor suppressor (TS) genes and the two-hit hypothesis. *Nature Ed.* 2008;1(1):177. Available at: <https://www.nature.com/scitable/topicpage/tumor-suppressor-ts-genes-and-the-two-887>
- Moolgavkar SH, Venzon DJ. Two-event models for carcinogenesis: incidence curves for childhood and adult tumors. *Math Biosci.* 1979;47(1-2):55-77. doi:10.1016/0025-5564(79)90005-1.
- Moolgavkar SH, Knudson AG Jr. Mutation and cancer: a model for human carcinogenesis. *J Natl Cancer Inst.* 1981;66(6):1037-1052. doi:10.1093/jnci/66.6.1037.
- Moolgavkar SH. Model for human carcinogenesis: action of environmental agents. *Environ Health Perspect.* 1983;50:285-291. doi: 10.1289/ehp.8350285.
- Moolgavkar SH. Biologically motivated two-stage model for cancer risk assessment. *Toxicol Lett.* 1988;43(1-3):139-150. doi:10.1016/0378-4274(88)90025-2.
- Moolgavkar SH, Dewanji A, Venzon DJ. A stochastic two-stage model for cancer risk assessment. 1. The hazard function and the probability of tumor. *Risk Anal.* 1988;8(3):383-392. doi:10.1111/j.1539-6924.1988.tb00502.x.
- Moolgavkar SH, Dewanji A, Luebeck G. Cigarette smoking and lung cancer: a reanalysis of the British doctors' data. *J Natl Cancer Inst.* 1989;81(6):415-420. doi:10.1093/jnci/81.6.415.
- Moolgavkar S, Luebeck G. Two-event model for carcinogenesis: biological, mathematical, and statistical considerations. *Risk Anal.* 1990;10(2):323-341. doi:10.1111/j.1539-6924.1990.tb01053.x.
- Leubeck EG, Moolgavkar SH. Stochastic analysis of intermediate lesions in carcinogenesis experiments. *Risk Anal.* 1991;11(1):149-157. doi:10.1111/j.1539-6924.1991.tb00585.x.
- Heidenreich WF, Leubeck EG, Moolgavkar SH. Some properties of the hazard function of the two-mutation clonal expansion model. *Risk Anal.* 1997;17(3):391-399. doi:10.1111/j.1539-6924.1997.tb00878.x.
- Leubeck EG, Heidenreich WF, Hazelton WD, Paretzke HG, Moolgavkar SH. Biologically based analysis of the data for the Colorado uranium miners cohort: age, dose and dose-rate effects. *Radiat Res.* 1999;152(2):339-351. doi:10.2307/3580219.
- Leubeck EG, Curtius K, Jeon J, Hazelton WD. Impact of tumor progression on cancer incidence curves. *Cancer Res.* 2013;73(3):1086-1096. doi:10.1158/0008-5472.CAN-12-2198.
- Bogen KT. Mechanistic models fit to ED001 data on >40,000 trout exposed to dibenzo[a, f]pyrene indicate mutations do not drive increased tumor risk. *Dose Response.* 2014;12(3):386-403. doi:10.2203/dose-response.13-019.Bogen.
- Bogen KT. A new theory of chemically induced tumorigenesis: key molecular events and dose-response implications. *Adv Molec Toxicol.* 2017;10:1-53. doi:10.1016/B978-0-12-804700-2.00001-5.
- Johnson NM, Egner PA, Baxter VK, et al. Complete protection against aflatoxin B(1)-induced liver cancer with a triterpenoid: DNA adduct dosimetry, molecular signature, and genotoxicity threshold. *Cancer Prev Res (Phila).* 2014;7(7):658-665. doi:10.1158/1940-6207.CAPR-13-0430.
- NCI. *SEER Cancer Statistics Review (CSR) 1975-2014. April 2, 2018. U.S. Surveillance, Epidemiology, and End Results (SEER) Program.* Bethesda, MD: National Cancer Institute (NCI), 2018. Tables 2.7-27. Available at: https://seer.cancer.gov/archive/csr/1975_2014/results_merged/sect_01_overview.pdf (accessed June 1, 2018).
- Friedrich T, Schellhaas H. Computation of the percentage points and the power for the two-sided Kolmogorov-Smirnov one sample test. *Statistical Papers.* 1998;39(4):361-375.
- ISO. *ISO 10312:1995(E), Ambient Air - Determination of Asbestos Fibres - Direct-Transmission Electroscopy Method (Table F.1 - Upper and Lower Limits of the Poissonian 95% Confidence Interval of a Count).* Genève, Switzerland: Author; 1995.
- Wolfram Research. *Wolfram Language and System Documentation Center.* Champaign, IL: Wolfram Research; 2019. (www.wolfram.com), <http://reference.wolfram.com/language/>
- NTP. *NTP Historical Controls Report All Routes and Vehicles: F 344/N RATS.* National Toxicology Program (NTP), Research Triangle Park, NC, p. 21, 2013. Available at: http://ntp.niehs.nih.gov/ntp/historical_controls/ntp2000_2013/histcont2013_ratsf344_allroutes_508.pdf.
- Portier CJ, Hedges JC, Hoel DG. Age-specific models of mortality and tumor onset for historical control animals in the national toxicology program's carcinogenicity experiments. *Cancer Res.* 1986;46(9):4372-4378.
- Ettlin RA, Stirnimann P, Prentice DE. Causes of death in rodent toxicity and carcinogenicity studies. *Toxicol Pathol.* 1994;22(2):165-178. doi:10.1177/019262339402200210.
- Hertzog PJ, Lindsay Smith JR, Garner RC. A high pressure liquid chromatography study on the removal of DNA-bound aflatoxin B1 in rat liver and in vitro. *Carcinogenesis.* 1980;1(9):787-793.
- Croy RG, Wogan GN. Temporal patterns of covalent DNA adducts in rat liver after single and multiple doses of aflatoxin B1. *Cancer Res.* 1981;41(1):197-203.

30. Essigmann JM, Croy RG, Bennett RA, Wogan GN. Metabolic activation of aflatoxin B₁: patterns of DNA adduct formation, removal, and excretion in relation to carcinogenesis. *Drug Metab Rev.* 1982;13(4):581-602. doi:10.3109/03602538209011088.
31. Leadon SA, Tyrrell RM, Cerutti PA. Excision repair of aflatoxin B₁-DNA adducts in human fibroblasts. *Cancer Res.* 1981;41(12 Pt 1):5125-5129.
32. Bailey EA, Iyer RS, Stone MP, Harris TM, Essigmann JM. Mutational properties of the primary aflatoxin B₁-DNA adduct. *Proc Natl Acad Sci USA.* 1996; 93(4):1535-1539. doi:10.1073/pnas.93.4.1535.
33. Wang JS, Groopman JD. DNA damage by mycotoxins. *Mutat Res.* 1999;424(1-2):167-181.
34. Smela ME, Hamm ML, Henderson PT, Harris CM, Harris TM, Essigmann JM. The aflatoxin B₁ formamidopyrimidine adduct plays a major role in causing the types of mutations observed in human hepatocellular carcinoma. *PNAS.* 2002;99(10):6655-6660. doi:10.1073/pnas.102167699.
35. Sotomayor RE, Washington M, Nguyen L, Nyang'anyi R, Hinton DM, Chou M. Effects of intermittent exposure to aflatoxin B₁ on DNA and RNA adduct formation in rat liver: dose-response and temporal patterns. *Toxicol Sci.* 2003;73(2):329-338. doi:10.1093/toxsci/kfg076.
36. Alekseyev YO, Hamm ML, Essigmann JM. Aflatoxin B₁ formamidopyrimidine adducts are preferentially repaired by the nucleotide excision repair pathway in vivo. *Carcinogenesis.* 2004;25(6):1045-1051. doi:10.1093/carcin/bgh098.
37. Bedard LL, Alessi M, Davey S, Massey TE. Susceptibility to aflatoxin B₁-induced carcinogenesis correlates with tissue-specific differences in DNA repair activity in mouse and in rat. *Cancer Res.* 2005;65(4):1265-1270. doi:10.1158/0008-5472.CAN-04-3373.
38. Bedard LL, Massey TE. Aflatoxin B₁-induced DNA damage and its repair. *Cancer Lett.* 2006;241(2):174-183. doi:10.1016/j.canlet.2005.11.018.
39. Besaratinia A, Kim SI, Hainaut P, Pfeifer GP. In vitro recapitulating of TP53 mutagenesis in hepatocellular carcinoma associated with dietary aflatoxin B₁ exposure. *Gastroenterol.* 2009;137(3):1127-1137, 1137.e1-5. doi:10.1053/j.gastro.2009.06.002.
40. Woo LL, Egner PA, Belanger CL, et al. Aflatoxin B₁-DNA adduct formation and mutagenicity in livers of neonatal male and female B6C3F₁ mice. *Toxicol Sci.* 2011;122(1):38-44. doi:10.1093/toxsci/kfr087.
41. Lin YC, Li L, Makarova AV, Burgers PM, Stone MP, Lloyd RS. Molecular basis of aflatoxin-induced mutagenesis-role of the aflatoxin B₁-formamidopyrimidine adduct. *Carcinogenesis.* 2014; 35(7):1461-1468. doi:10.1093/carcin/bgu003.
42. Vartanian V, Minko IG, Chawanthayatham S, et al. NEIL1 protects against aflatoxin-induced hepatocellular carcinoma in mice. *Proc Natl Acad Sci USA.* 2017;114(16):4207-4212. doi:10.1073/pnas.1620932114.
43. Zeise L, Wilson R, Crouch EA. Dose-response relationships for carcinogens: a review. *Environ Health Perspect.* 1987;73: 259-306.
44. Buss P, Caviezel M, Lutz WK. Linear dose-response relationship for DNA adducts in rat liver from chronic exposure to aflatoxin B₁. *Carcinogenesis.* 1990;11(12):2133-2135.
45. Choy WN. A review of the dose-response induction of DNA adducts by aflatoxin B₁ and its implications to quantitative cancer-risk assessment. *Mutat Res.* 1993;296(3):181-198. doi:10.1016/0165-1110(93)90010-K.
46. Kaden DA, Call KM, Leong PM, Komives EA, Thilly WG. Killing and mutation of human lymphoblast cells by aflatoxin B₁: evidence for an inducible repair response. *Cancer Res.* 1987; 47(8):1993-2001.
47. Maier P, Schawalder HP. Hepatocarcinogens induce gene mutations in rats in fibroblast-like cells from a subcutaneous granulation tissue. *Carcinogenesis.* 1988;9(8):1363-1368.
48. Preisler V, Caspary WJ, Hoppe F, Hagen R, Stopper H. Aflatoxin B₁-induced mitotic recombination in L5178Y mouse lymphoma cells. *Mutagenesis.* 2000;15(1):91-97. doi:10.1093/mutage/15.1.91.
49. Stettler PM, Sengstag C. Liver carcinogen aflatoxin B₁ as an inducer of mitotic recombination in a human cell line. *Mol Carcinog.* 2001;31(3):125-138.
50. Wiemels J. Perspectives on the causes of childhood leukemia. *Chem Biol Interact.* 2012;196(3):59-67. doi:10.1016/j.cbi.2012.01.007.
51. Greaves M. A causal mechanism for childhood acute lymphoblastic leukaemia. *Nature Rev Cancer.* 2018;18(8):471-484, 526. doi:10.1038/s41568-018-0015-6.
52. Touati E, Michel V, Thiberge JM, et al. Deficiency in OGG1 protects against inflammation and mutagenic effects associated with *H. pylori* infection in mouse. *Helicobacter.* 2006;11(5): 494-505. doi:10.1111/j.1523-5378.2006.00442.x.
53. Chiba T, Marusawa H, Ushijima T. Inflammation-associated cancer development in digestive organs: mechanisms and roles for genetic and epigenetic modulation. *Gastroenterology.* 2012; 143(3):550-563. doi:10.1053/j.gastro.2012.07.009.
54. Fedeles BI, Freudenthal BD, Yau E, et al. Intrinsic mutagenic properties of 5-chlorocytosine: A mechanistic connection between chronic inflammation and cancer. *Proc Natl Acad Sci USA.* 2015;112(33): E4571-E4580. doi:10.1073/pnas.1507709112.
55. Hahn MA, Hahn T, Lee DH, et al. Methylation of polycomb target genes in intestinal cancer is mediated by inflammation. *Cancer Res.* 2008;68(24):10280-10289. doi:10.1158/0008-5472.CAN-08-1957.
56. Calabrese EJ. The additive to background assumption in cancer risk assessment: a reappraisal. *Environ Res.* 2018;166:175-204. doi:10.1016/j.envres.2018.05.015.
57. Moffat I, Chepelev N, Labib S, et al. Comparison of toxicogenomics and traditional approaches to inform mode of action and points of departure in human health risk assessment of benzo[*a*]pyrene in drinking water. *Crit Rev Toxicol.* 2015;45(1):1-43. doi: 10.3109/10408444.2014.973934.
58. Ruetze M, Gallinat S, Wenck H, Deppert W, Knott A. In situ localization of epidermal stem cells using a novel multi epitope ligand cartography approach. *Integr Biol (Camb).* 2010;2(5-6): 241-249. doi:10.1039/b926147 h.

-
59. Rennert RC, Sorkin M, Garg RK, Gurtner GC. Stem cell recruitment after injury: lessons for regenerative medicine. *Regen Med.* 2012; 7(6):833-850. doi:10.2217/rme.12.82.
 60. Buckley SM, Delhove JM, Perocheau DP, et al. In vivo bioimaging with tissue-specific transcription factor activated luciferase reporters. *Sci Rep.* 2015;5:11842. doi:10.1038/srep11842.
 61. Iwano S, Sugiyama M, Hama H, et al. Single-cell bioluminescence imaging of deep tissue in freely moving animals. *Science.* 2018;359(6378):935-939. doi:10.1126/science.aaq1067.
 62. López-Lázaro M. The stem cell division theory of cancer. *Crit Rev Oncol/Hematol.* 2018;123:95-113. doi:10.1016/j.critrevonc.2018.01.010.